ORIGIN AND SEQUENTIAL DEVELOPMENT OF BADENIAN-SARMATIAN CLINOFORMS IN THE CARPATHIAN FORELAND BASIN (SE POLAND)

SZCZEPAN J. PORĘBSKI[1], KAJA PIETSCH[2], RYSZARD HODIAK[2] and RONALD J. STEEL[3]

[1]Institute of Geological Sciences, Kraków Research Centre, Polish Academy of Sciences, Senacka 1, 31-002 Kraków, Poland; ndporebs@cyf-kr.edu.pl
[2]Department of Geology, Geophysics and Environmental Protection, Academy of Mining and Metallurgy, Al. Mickiewicza 30, 30-059 Kraków, Poland
[3]University of Wyoming, Department of Geology and Geophysics, Laramie, Wyoming, 82071, USA

Abstract: Upper Badenian-lower Sarmatian (Miocene) strata along the active (southern) margin in the Carpathian Foreland Basin reveal seismic-scale deltaic clinoforms that grew from the south and developed a shelf-to-basin floor relief of over 300 m. Two architectural types and six 4th-order sequences were distinguished along the clinoforms on the basis of correlation of an extensive network of seismic lines and geophysical well logs. A Type A clinoform consists of steeply dipping (3–4°), planar-oblique strata that occur in narrow (2–4 km wide) belts composed chiefly of aggrading thick-bedded massive sandstones with onlap upper terminations. Type B clinoforms occur in wide (8–12 km) belts of less steep (≤2°), strongly tangential strata composed of mouth-bar/prodeltaic increments that lack thick turbidites and show down-ward-stepping to retrogradational stratal arrangements. Both clinoform types document shelf-margin accretion, chiefly during periods of relative sea-level fall and early rise. None of these types predicts a coeval basin-floor fan development, either because the slope was too narrow to ignite delta-fed hyperpycnal flows into high-efficiency turbidity currents (type A), or the bulk of the sand delivered to the shelf edge was trapped within slope-perched mouth bars shifting 6–10 km around the freshly formed shelf margin (Type B) during relative-sea level oscillations. The lower three sequences (upper Badenian) reveal a strong aggradational component, whereas starting from the angular unconformity at base of the Anomalinoides dividens Zone (lower Sarmatian) the offlap break assumes an increasingly flat trajectory basinwards. This change is thought to reflect a decreased rate of addition of accommodation due to cessation of thrust loading, and faster progradation of the clinoform. It is concluded that large-scale clinoformed shelf margins are not limited to rifted continental shelf margins, but can also be present in foreland basins. In such an environment, flexural and fault-induced subsidence promotes long-term relative sea-level rise in the hangingwall and, consequently, the generation of long and high deltaic clinoforms on the accreting shelf margin, whereas the actively rising footwall precludes the preservation of paralic facies and provides an abundant sediment supply for delta growth.

Key words: Western Carpathians, Carpathian Foreland Basin, clinoform, shelf-margin delta.

Introduction

Although Miocene deposits in the Carpathian Foreland Basin (Fig. 1) have been the subject of vigorous research for many decades, an understanding of their sedimentary environments and depositional architectures has developed rather slowly. The conventional view of these deposits as molasse has led to the erroneous belief in their invariably shallow-water origin. Whereas this is essentially true for Miocene basin fill along the cratonward (northern) side of the basin (e.g. Czapowski 1994; Kasprzyk 1993; Roniewicz & Wysocka 1999), there is growing evidence of repeated development of a marked bathymetric gradient downdip of the active (southern) margin. The evidence includes the presence of Badenian submarine fans (Maksym et al. 1997), shallow neritic to bathyal foraminiferal assemblages (Czepiec & Kotarba 1998; Gonera 1994), and seismic-scale clinoforms (Krzywiec 1997). Evidence presented earlier (Porębski 1999) and expanded here has shown that these clinoforms descended from the south and developed a shelf-to-basin floor relief 300–400 m in height. Similar clinoforms are associated with the shelf break of Quaternary continental margins (e.g. McMaster et al. 1970; Suter & Ber-

ryhill 1985; Tesson et al. 2000), but can also be an important constituent of any delta-fed subaqueous platforms located at the margins of rapidly subsiding marine basins (Porębski & Steel in press). Deltaic clinoforms that grew onto bathyal slopes have, surprisingly, rarely been reported from the pre-Quaternary record; notable exceptions include examples described by Mayall et al. (1992), Steel et al. (2000) and Blink-Bjorklund et al. (2001).

The main goals of the present work are (1) to reconstruct clinoform architecture via detailed geophysical log and seismic correlations, in order to get insight into the evolution of such clinoformed active margins and (2) to better asses the role of shelf-margin deltas as the potential staging areas for supply of sand to the deep sea.

Regional setting

The studied succession is located within the outermost, little to non-deformed unit of the Carpathian orogenic belt (Fig. 1), which formed the peripheral part of the Carpathian foreland basin system. This system was generated on the interior side
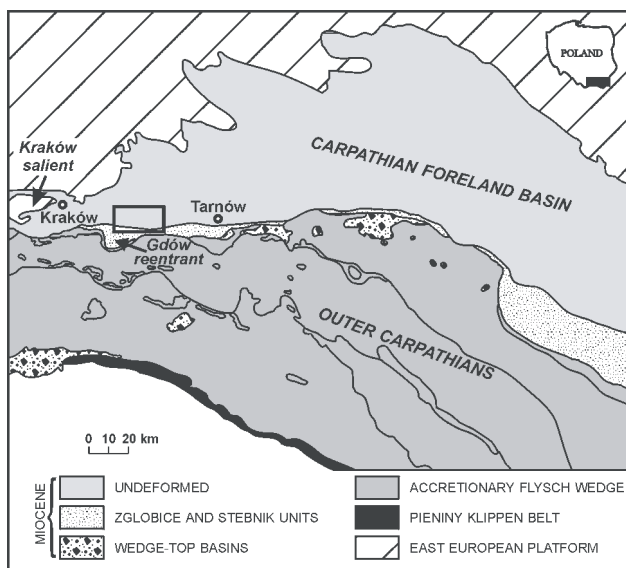
Fig. 1. Map showing the location of study area (rectangle) within the geological framework of the Carpathians.

of a collision zone during lithospheric flexure of the East European Platform in response to a northward-stepping thrust load (Kotlarczyk 1985; Oszczypko & Żytko 1987; Oszczypko 1997). The Miocene fill of the Carpathian Foreland Basin is up to 3.5 km thick, and consists of deep-water, shallow-marine and deltaic siliciclastic sediments and evaporites. In addition to its northerly progradation, the basin fill shows also a large-scale offlap and thickness increase towards the east along the convergent margin (Ney 1968), reflecting an increased accommodation in that direction. Such a pattern may possibly indicate either an easterly increase in loading along the strike of fold-thrust belt or, together with *an echelon* orientation of Outer Carpathian nappes, the creation of tectonic accommodation due mainly to a left-lateral transpression. Cratonwards, individual clinothem bodies onlap a south-dipping unconformity with an associated hiatus that embodies the Paleocene–early Oligocene (e.g. Żytko 1999). The hiatus spans the main subsidence phases in the foreland basin, but the thrust loading continued through Miocene time, giving rise to flexural subsidence in the basin (Oszczypko 1997). The unconformity surface follows a regional, SE-draining valley system extending across the entire cratonic margin, with valley relief locally up to 1000 m (Karnkowski & Ozimkowski 2001). This craton-sourced system was active mainly during the underfilled phase of foreland development (e.g. Picha 1996) and possibly during the early Badenian (Połtowicz 1998), but remained largely dormant during late Badenian–Sarmatian time (Krzywiec 1999; Porębski 1999).

Study area

Structural setting

The study area, extending some 50 km along strike and 30 km downdip, is located immediately east of the Krakow salient (Ney 1968) and north of the main Carpathian over-thrust (Figs. 1 and 2). Along this thrust, flysch rocks together with a narrow strip of Miocene sediments, are superposed onto the weakly to non-deformed Miocene basin fill. Within the study area, the fill is up to 1300 m thick and consists mainly of thin-bedded sandstones, siltstones and mudstones intercalated with thicker sandstone tongues. Seismic mapping has shown that the pre-Miocene cratonic basement dips ca. 3° southeastwards (Fig. 3), and is dissected by the Szczurowa paleovalley (Połtowicz 1998). The valley is up to 4 km wide and 400 m deep in the southeast; towards the NW, it shallows and splits into three branches, each less than 0.5 km in width (Fig. 3).
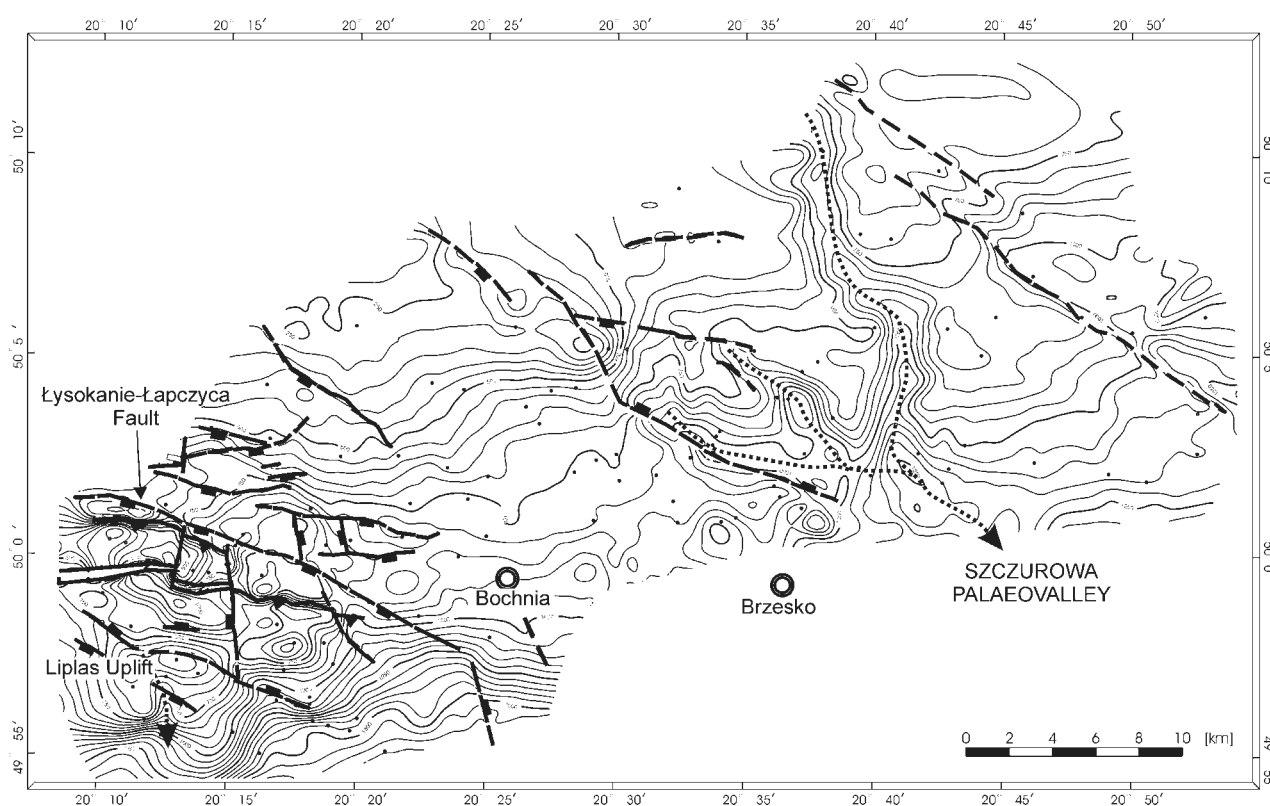
The basement is affected by extensional and possibly strike-slip faults. Major faults trend NW-SE, downthrowing mainly to the SW. Minor faults strike NNW-SSE and show different throw directions. Along the main fault zone in the area, referred to as the Łysokanie-Łapczyca fault (Fig. 3), the basement was displaced 250–370 m southwards. During Sarmatian compression, this fault formed a frontal ramp on which older Miocene sediments, together with slivers of the basement, were detached and formed a steeply dipping, NNE-verging anticlinal thrust stack. Another stack forms the core of the Liplas uplift farther to the SW (Fig. 3). Both stacks continue eastwards into a narrow band of folded and faulted Miocene sediments, and all together are distinguished as the Zgłobice Unit (Kotlarczyk 1985). The unit is bordered to the south by the main Carpathian overthrust. South of the Łysokanie-Łapczyca fault, the Zgłobice Unit expands in width within the Gdów re-entrant which is defined by a southerly deflection in the overall W-E striking Carpathian overthrust (Fig. 2). The clinoform body that escaped deformation extends north of the Zgłobice Unit, and shows a structural tilt of 1–2° NE.
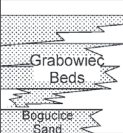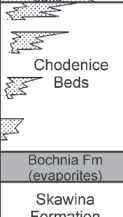
Stratigraphy

The succession is split by an evaporite unit (Fig. 4) that is distinguished as the Bochnia Formation (Kuciński 1982) and forms an excellent correlative horizon traceable across almost the entire basin. Although the Bochnia Formation was later redefined to include gypsum and anhydrite within the Krzyżanowice Formation (Alexandrowicz 1997) and halite within the Wieliczka Formation (Garlicki 1994), such a two-fold subdivision cannot be used consistently in the subsurface work and, hence, is not followed here. Evaporite rocks in the southern part of the basin provide numerous signs of gravity collapse (Ślączka & Kolasa 1997) and are considered to represent deep-water facies (Peryt 2000), whereas those exposed along the cratonic margin are arranged in a number of upward-shallowing cycles with evidence of subaerial exposure (Kasprzyk 1993). The evaporite unit is overlain by 20–300 m of shales, mudstones, sandstones and tuffs of the Chodenice Beds (Fig. 4) that are unconformably followed up by the more sandy Grabowiec Beds, 300–500 m thick. Both units thin basinwards within shales of the Machów Formation (Jasionowski 1997), and are replaced along the northern basin margin by a thin stack of transgressive–regressive cycles comprised of mixed, siliciclastic-carbonate nearshore to basinal deposits (Chmielnik Formation and equivalents; Czapowski 1994; Roniewicz & Wysocka 1999).
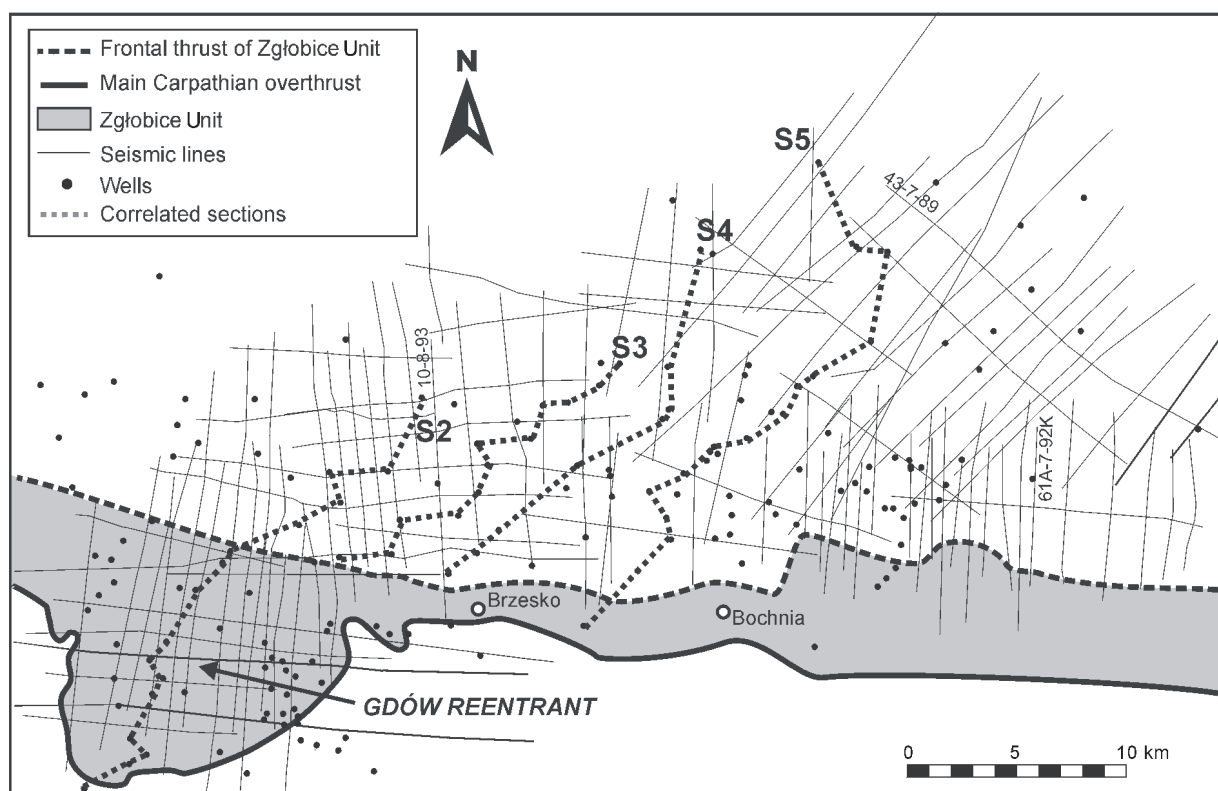
Fig. 2. Index maps showing the locations of seismic lines, wells and correlation sections.

Fig. 3. Depth-map of the top of cratonic basement below the offlaping Miocene succesion. The basement is dissected by the southeasterly plunging valleys (dotted) and is affected by extensional and strike-slip faults. The faults in the southwestern corner formed ramps for thrusts during the latest Badenian compression.

Stage	Lithostratigraphy	Depositional sequences		Main correlation surfaces	Biostratigraphy		
		3rd-ord.	4th-ord.		Kirchner, 1956	Foraminiferal zones (*)	Nannoplankton zones (**)
SARMATIAN	Grabowiec Beds	Sa1	S6	Sb7	6 (Bulimina-bearing)	Anomallnoides dividens	NN6
			S5	SB6			
				MFS5			
				SB5			
	Bogucice Sand		S4	MFS4			
				SB4au			
BADENIAN	Chodenice Beds	Ba2	S3	MFS3	5	Hanzawaia crassiseptata	
				SB3	4c (Globigerina-bearing)	Neobulimina longa	
			S2	MFS2			
				SB2			
			S1	MFS1	4b (Radiolaria bearing)		
				SB1			
	Bochnia Fm (evaporites)			MFS0	3	Uvigerina costai	
	Skawina Formation				2	Candorbulina universa	NN5
				Mau	1		

●— Incised valley

Fig. 4. Stratigraphic scheme of Miocene succession in the study area, showing the sequence stratigraphic subdivision against the biostratigraphic framework. (*) — after Łuczkowska (1964, 1995), Czepiec & Kotarba (1998), Olszewska (1999); (**) — after Garecka & Jugowiec (1999). MFS — maximum flooding surface; SB — sequence boundary; *au* — angular unconformity; M*au* — base-of-Miocene unconformity.

The supra-evaporite succession, discussed here, comprises three local forminiferal zones corresponding to the NN6 Nannoplankton Zone, and is probably not much more than 1 Ma in duration (Fig. 4). Absolute Ar/Ar dating of a hornblende tuff located near the base of the Bochnia Formation has yielded equivocal results of 11–28 Ma (Bukowski 1999).

Material and methods

In total, about 110 seismic lines, and geophysical logs from ca. 160 wells provided by Polish Oil and Gas Co., were used in the present study (Fig. 2). The available seismic grid extends some 20 km downdip; dip and strike line spacings over most of the mapped area are 0.5–2 km. The vertical resolution does not generally extend below 20 m. Because of the scarcity and poor preservation of core material, information from small and scattered outcrops was also used, giving a better insight into facies development. Unconformities defined by different stratal lapouts and erosional truncations on seismic sections were traced as close as possible to geophysical wells (gamma-ray, resistivity, neutron-porosity, spontaneous potential). Such correlations aided by stacking patterns recognized on well logs, were used to define key surfaces (maximum transgression and regression surfaces, erosional unconformities and their correlative conformities). These formed a basis for the definition and mapping of depositional systems tracts (geometry, thickness and net sand contents) and the unravelling the paleogeographic evolution of the studied margin for selected time slices.

Seismic data interpretation, time/depth conversions and seismostratigraphic mapping were carried out using Schlumberger's GeoFrame 3.8.1 package for 2D seismic interpretation (Charisma). Well log correlation and mapping of stratigraphic attributes were performed using Landmark's StratWorks module. Seismic data are of different vintages (1978–1993) and, hence, of variable quality. In order to standardise and improve the quality of seismic data, an advanced reprocessing scheme using the Omega system was applied to selected sections. The crucial element in the reprocessing, which was done by Geofizyka-Kraków Ltd., involved (1) the application of COHERENCY STACK and the RNA procedures that improved signal/noise ratio (S/N); (2) the frequency-distance migration F-X that enhanced the horizontal resolution, particularly in tectonically disturbed segments; and (3) the application of wavelet processing that permitted the acquisition a zero-phase record that is especially useful for extracting stratigraphic information from seismic data. The reprocessed sections, with real amplitude relationships preserved, were hung on the common reference level set up at 170 m a.s.l.

Clinoforms

Geometry

Seismic sections reveal the presence of a large-scale clinoformed body that descends towards the north and appears to wedge out by onlap onto the top of the Bochnia evaporites dipping southwards (Figs. 5 and 6). However, a closer inspection of these relationships shows that the top of the Bochnia Formation does not represent a single onlap unconformity. The body consists of a series of clinothems that thin north- and northeastwards towards the basin centre, and are bounded by lap-out unconformities. The lower ends of successive basinward clinothems do not abut onto the evaporite top. Instead, they tend to wedge out basinwards at progressively higher levels above this surface forming a thin zone of ascending contacts corresponding to condensed, shale-prone sediments.

Clinothem reflectors in the landward (southern) side of the clinoform body are planar with short angular to tangential lower ends and can have truncated tops. Basinwards, successive clinothem bundles assume more tangential shapes with long, locally hummocky toes and grade occasionally into sigmoidal forms. The latter display well-developed offlap breaks that mark the change in declivity at the top of the prograding sediment prism. Clinoform slopes dip generally at 2–3°, but locally the steepest, upper segments in planar reflectors can reach 4–6° in inclination. The maximum height that the slope attains is 330 m, but smaller-scale clinoform bodies (mouth bars or deltas) perched on the main slope rarely exceed several tens of metres in amplitude (Fig. 6). Upper clinoforms segments are almost invariably associated with the most sand-prone sediment (Fig. 5). These shelf-edge sandbodies generally tend to pinch out landwards within a more heterolithic facies.

The well-developed slope break is backed by a flat to gently N-dipping platform (shelf) that can be locally incised by N to NE-trending channels, 0.5–1 km wide (Fig. 7F). The preserved width of the shelf between the successive offlap breaks and the frontal thrust of the Zgłobice Unit does not exceed 8 km, but it may be far greater in the uppermost 100–150 m of the succession that has not been seismically imaged. Although clearly progradational in character, the clinoform set reveal a strong aggradational component reflected in the rising to land-

ward-stepping trajectory of the offlap breaks (Fig. 5). Internally, the clinoform set reveal a number of downlap and onlap unconformities that are particularly discernible within the slope reaches of the shelf-margin succession (Fig. 6) and have been used for subdivision of the studied succession into depositional sequences.

Facies spectrum

The main features of the clinoform prism include:
• Major sandbodies are mainly strike-oriented and they tend to wedge both landwards (to the S) and basinwards (to the N) within marine mudstones and shales (Fig. 5);
• The maximum sand development tends to be associated with the shelf edge or offlap break (Fig. 5);
• Fine-grained sediment provides microfossil assemblages of bathyal, neritic, nearshore to freshwater aspects (e.g. Gonera 1994; Czepiec & Kotarba 1998; Gedl 1998, unpublished; Olszewska 1999);

• Sands include both classical and high-density turbidites, deltaic mouth bars, and shell-bearing, cross-bedded shoreface sandstones (Porębski & Oszczypko 1999; Porębski 1999) (Fig. 8);
• There is little, if any, evidence of coastal plain (paralic) facies.

Facies landwards of the offlap break: Valley and other channel fills are typified by a blocky to bell-shaped gamma-ray response and vary in thickness from 5 to 55 m. They consist of medium-grained, locally conglomeratic sand and poorly consolidated sandstones that are massive or display large-scale trough cross-stratification associated with mollusc detritus. They are interbedded with intraclasts breccias and dm-thick heterolithic beds (Fig. 8A). A valley recognized on a strike-oriented seismic section shown in Fig. 9, is 5 km wide and displays a compound fill, up to 60 m thick, with clearly recognizable lateral accretion strata. Either a fluvial or estuarine origin can be inferred for this valley fill. Some cross-bedded shell-bearing sandstones may represent sharp-based
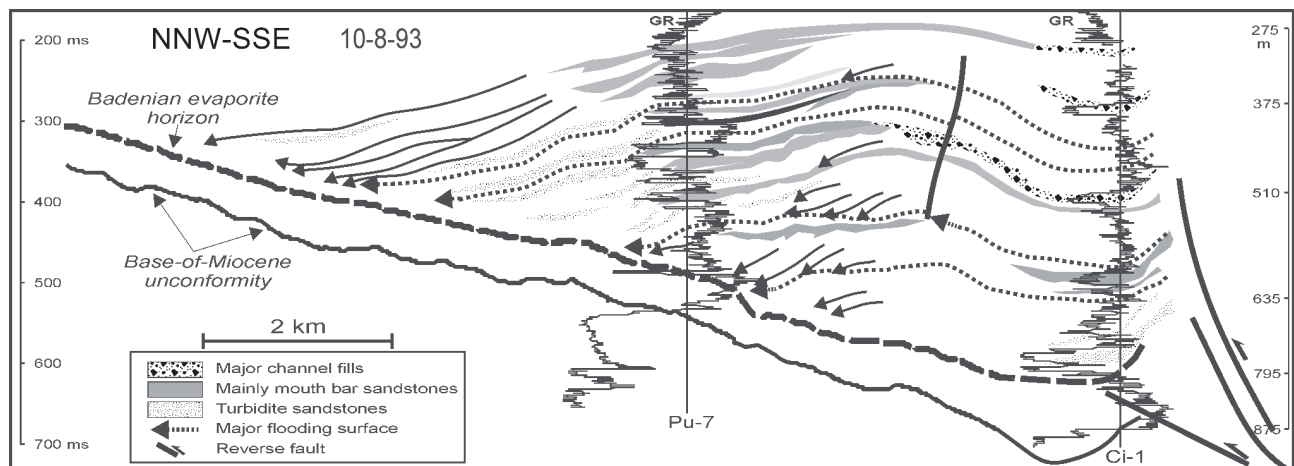

Fig. 5. Interpreted dip-oriented seismic line showing the concentration of sand bodies along the accreting shelf edge.
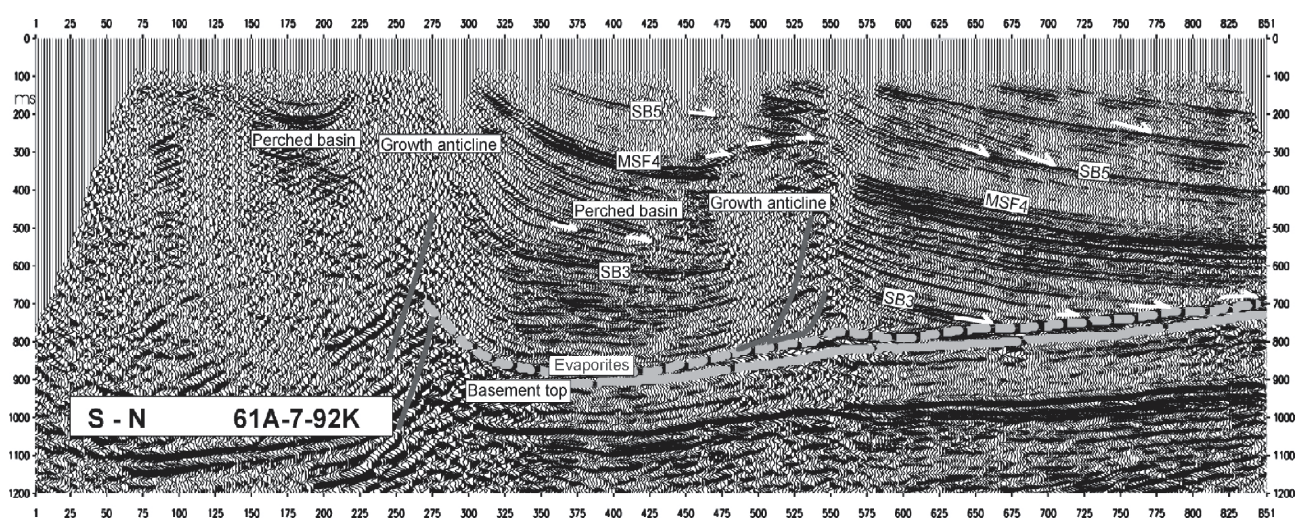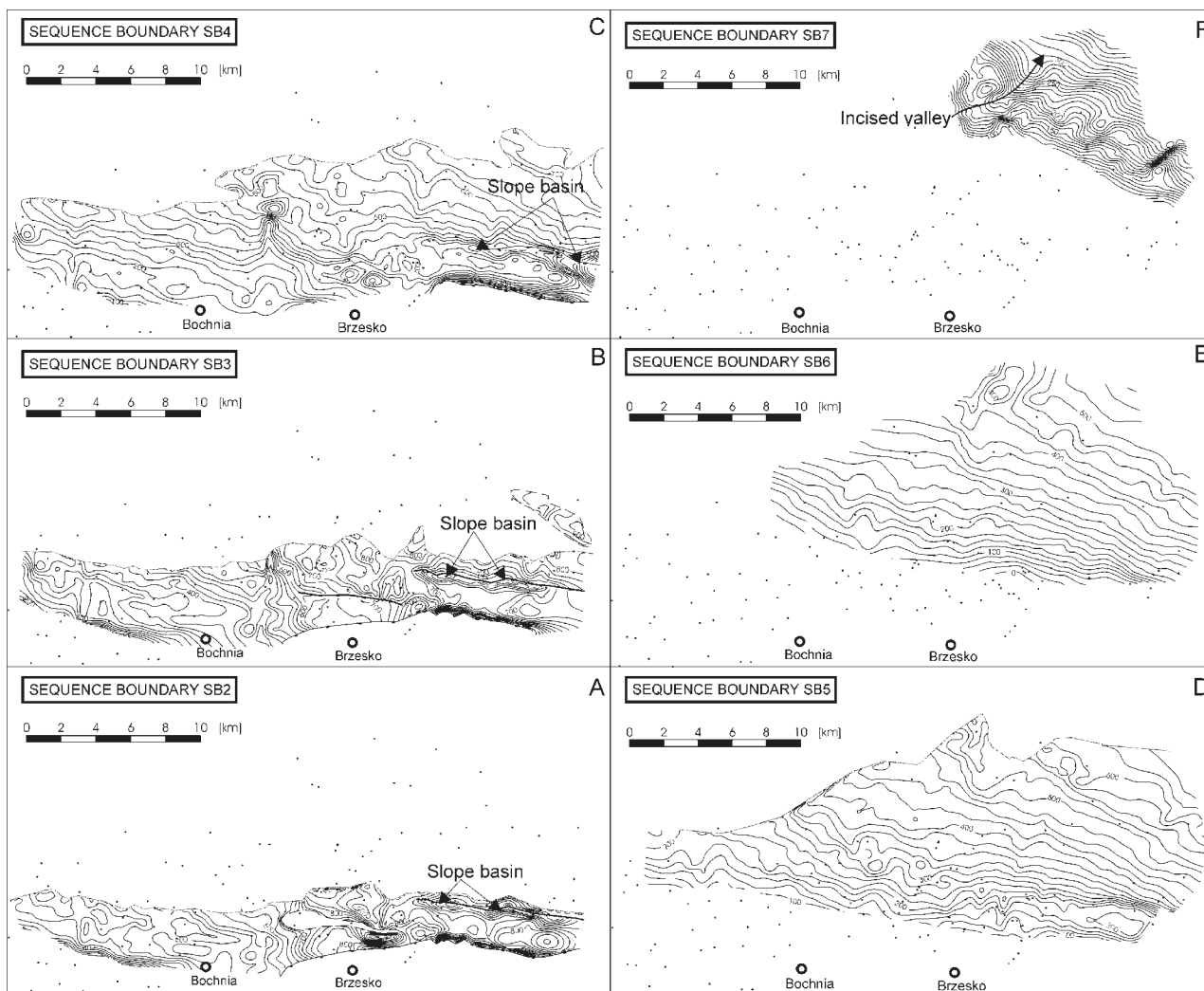

Fig. 6. Seismic dip-section showing the growth anticlines and associated mini-basins within the clinoform that is backed southwards by deformed Miocene sediments.

Fig. 7. Time maps showing the evolution of the prograding clinoform geometry along selected sequence boundaries and their correlative conformities. Note a valley breaching the shelf along unconformities SB3 (B) and SB7 (F), and the growth anticlines with intervening slope basins in (A–C).

shoreface facies, as suggested by the bimodal dip directions of cross-sets, with the modes directed towards the NE (basin-wards) and SSE (Porębski & Oszczypko 1999).

Mouth-bar facies form upward-coarsening units that are usually less than 20 m thick. They consist of non- to very weakly bioturbated laminated mudstones and linsen to wavy-bedded siltstone/very fine sandstone/mudstone heteroliths (Fig. 8C). The latter become interbedded upwards with dm thick, fine-grained Tbc turbidite sands. Upper levels of the mouth bar units reveal sharp-based fine- to medium-grained sandstones rich in plant detritus, which are predominantly rip-ple and flat laminated. The sandstones, 1–7 m thick, are com-monly extensively deformed into balls and pillows, but swa-ley and hummocky cross-stratifications is discernible in places. Mixtures of open-marine and fresh-water dinocysts are common in this facies (Gedl 1998, unpublished).

Lower-shoreface/prodeltaic shelf facies consists mainly of laminated to occasionally bioturbated mudstones interbedded with cm-thick, fine-grained graded sand beds. These com-monly show gutter casts, groves and prod marks that are

aligned generally W-E, i.e. parallel to the inferred shoreline trend, with the prods pointing to the easterly-directed geo-strophic storm currents.

Facies basinwards of the offlap break: Coarsening-upward units typified by gamma-ray response of a strongly serrated pattern passing upwards into a weakly serrated to blocky seg-ment, that are located at or just below the former shelf edge, are interpreted as deltaic mouths bars perched on the upper slope. These units vary in thickness from 30 to 75 m. The dominant lithotype comprises amalgamated beds of massive, fine- to medium-grained and granule-bearing sandstones that are occasionally rich in plant detritus, shell hash and redepos-ited foraminifers (Fig. 8B). Dm-thick intervals of inversely-graded bands (traction carpet), flat and ripple-lamination are common. Soft-sediment deformation includes large-convolu-tions near bed tops and metre-scale, basinward-verging imbri-cated shear planes.

Slope sediments with which these mouth bars interfinger consist of two main facies. (1) A fine-grained host is repre-sented by bioturbated mudstones interbedded with heterolith-
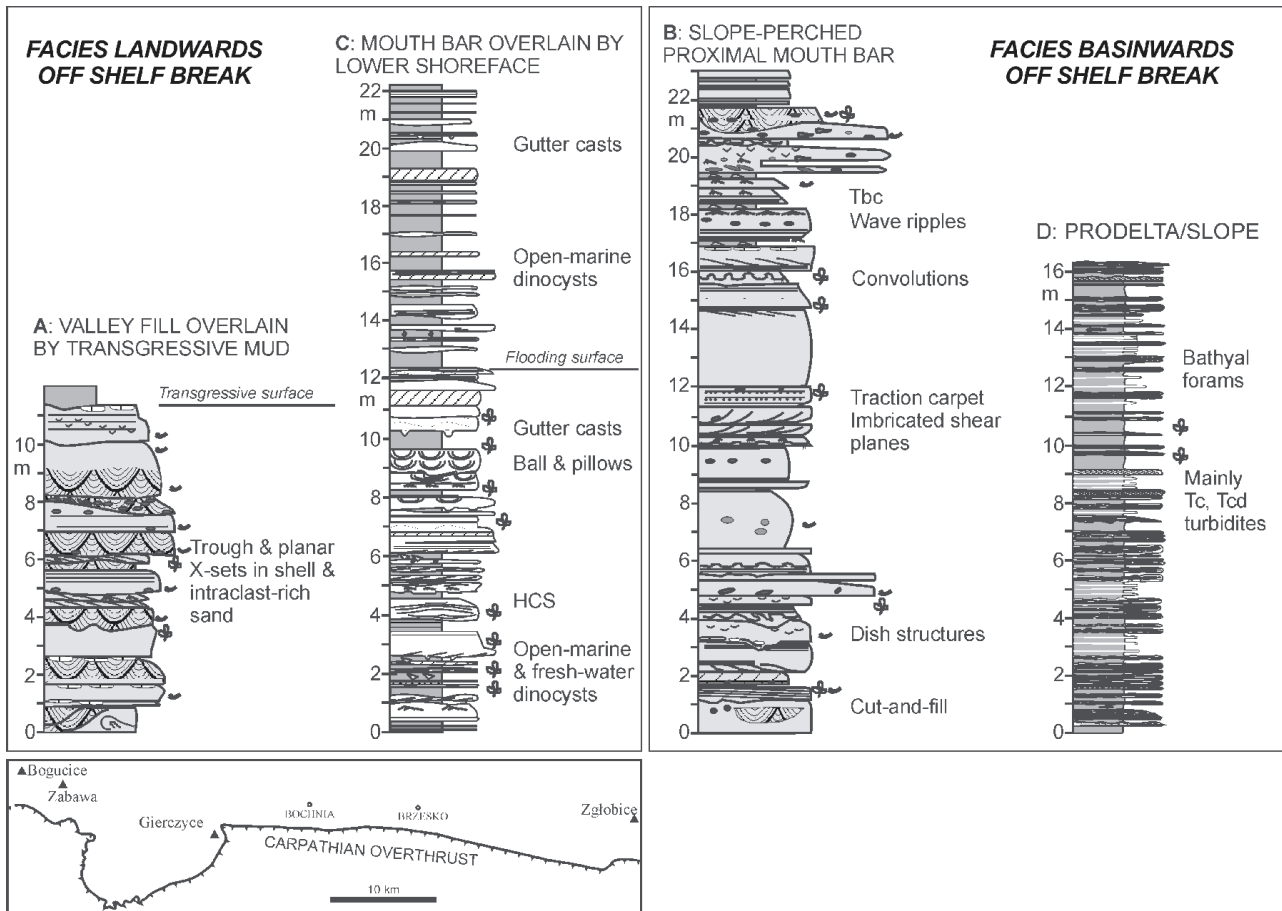
Fig. 8. Examples of outcrop logs showing facies differences between the shelf and slope segments in the delta (based on Porębski & Oszczypko 1999; Porębski 1999). A — Bogucice Sand, Bogucice; B — Bogucice Sand, Zabawa; C — Chodenice Beds, Zgłobice; D — Chodenice Beds, Gierczyce. Inset map show outcrop locations.
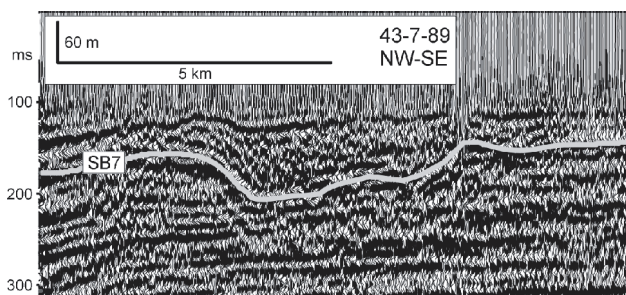
Fig. 9. Close-up view of seismic-strike section showing the compound fill of the valley associated with sequence boundary SB7.

ic packets that abound in very thin Tbc and Tcd sand turbidites (Fig. 8D). Thin-bedded sandstone/mudstone alternations display structures indicative of deposition from both waning and waxing turbulent suspensions, such as climbing ripples in normally graded and coarsening upwards sets. These fine-grained rocks are interbedded with (2) blocky sandstone units, 5–35 m thick, which are arranged either in progradational patterns, or occur in aggradational stacks, up to 125 m thick, with updip onlap terminations. Cores available from outside of the study area suggest that these sandstones are fine- to medium-grained and unstructured (massive) in character. Basinwards, these blocky sandstones, interpreted as the deposits of hyperpycnal flows, either terminate rather abruptly, or thin into heterolithic packets (5–25 m) which show a highly serrated gamma-ray response. The packets can possibly represent depositional lobes made of classical turbidites. Basin plain facies consists of shales and mudstones that locally contain concentrations of pelagic organisms, such as pteropods, foraminifers and radiolarians.

Paleoecological constraints

Although the paleobathymetric significance of Miocene microfossils from the Carpathian Foreland Basin has long been studied (e.g. Łuczkowska 1964, 1995; Gonera 1994; Czepiec & Kotarba 1998), discontinuous coring makes any precise bathymetric fluctuations difficult to detect in single vertical sections. However, the available results point to an overall upward shallowing throughout the studied clinoforms. Czepiec & Kotarba (1998) found that the Chodenice Beds abound in *Bulimina*, *Uvigerina*, and *Pulenia* ranging from bathyal depths (several hundreds of metres) to the outer shelf, whereas the lowermost Sarmatian deposits reveal high diversity miliolid-elphidiid and elphidiid-nonionid assemblages of more

shoreward aspects. This upward shallowing was associated with a decreasing salinity from normal marine to hyposaline levels, indicative of increased flux of freshwater (Czepiec & Kotarba 1998). The organic matter is dominated by type III kerogen (Kotarba et al. 1998), consistent with the postulated overall deltaic setting of the succession.

Evidence of syndepositional deformation

In the southeastern part of the study area clinoform slope is affected by two, parallel WNW-ESE striking blind thrusts with growth anticlines located above faults tips (Fig. 6). The thrust appears to flatten out southwards in a decollement plane merging into the evaporite unit. These anticlines define two, strike-elongated mini-basins perched on the slope. The basins are 1–1.5 km wide and 80–100 m deep, with their axes plunging gently eastwards (Fig. 7A–C). Fills include thick-bedded blocky sandstones and localized mouth bars. The formation of these growth structures appear to have post-dated the filling up of the Szczurowa Valley at its southern reach and came to an end before the development of unconformity SB5 (Figs. 4 and 10).
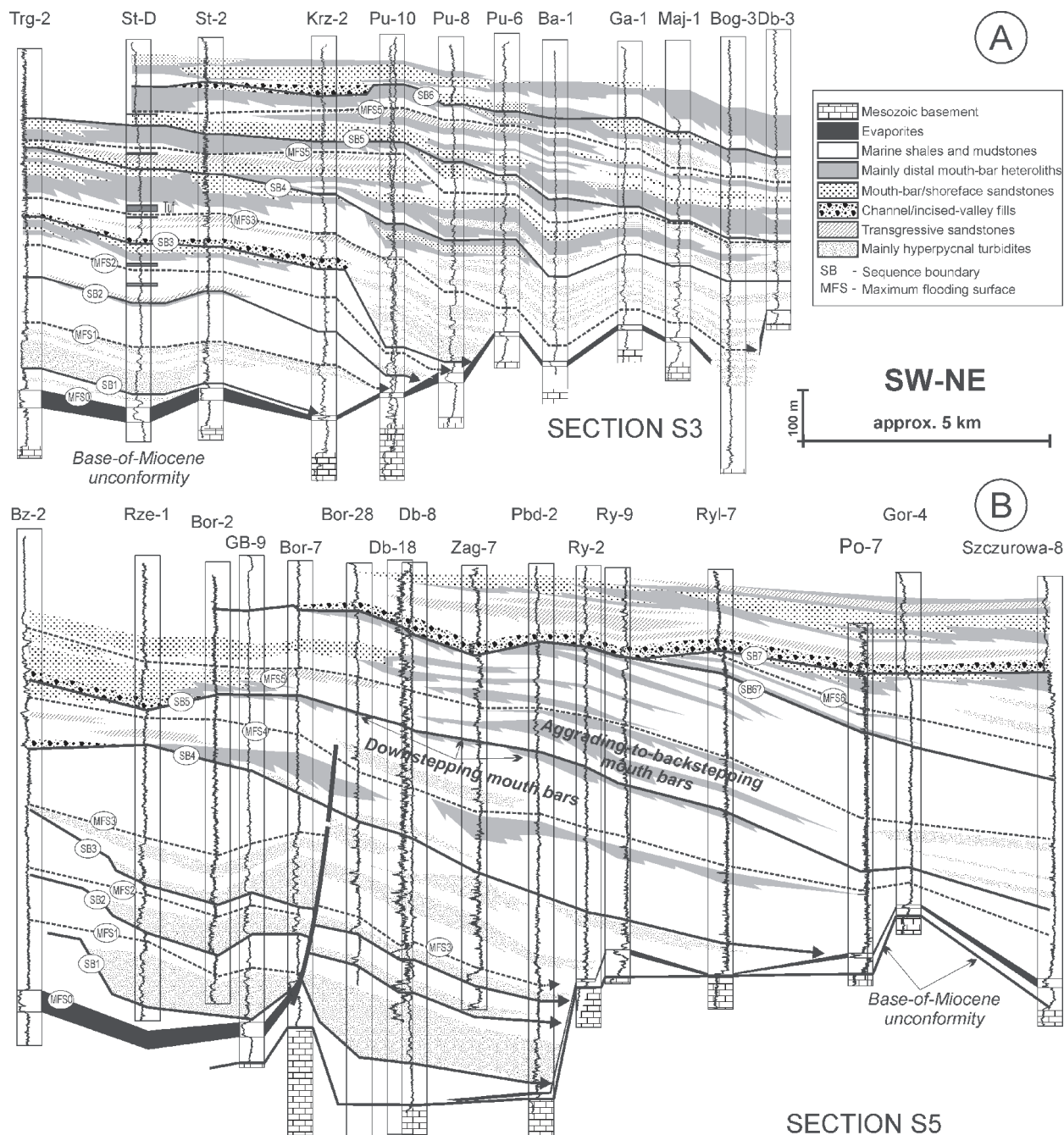
Fig. 10. Examples of log-based dip correlations with environmental interpretation added. Note thick-bedded, "blocky" sandstones in slope segments below sequence boundary SB4 and the downward-stepping to back stepping mouth bars perched on the slope.

Origin of the clinoforms

The existing interpretation of the clinoform body under consideration (e.g. Połtowicz 1997) is that it is a tectonic monocline developed above thrust faults. This interpretation is untenable in the light of the above evidence. In particular, it is inconsistent with (1) the presence of the distinct offlap breaks defining the platform-to-slope morphology and with, (2) the offlap geometry of the entire clinoform body, (3) a recurrent major sandbody development along the prograding offlap breaks, and with (4) the facies spectrum that documents a marked bathymetric gradient down the clinoforms. Hence, the observed topography is interpreted to reflect a shelf-slope-basin plain setting, i.e., a shelf margin that evolved in response to deltaic sediment delivery from the south. The nearly 400 m relief of the clinoform slope represents a reasonable minimum estimate of the paleowater column depth below the shelf break. This is compatible with the water depth range postulated on paleoecological ground (Czepiec & Kotarba 1998). The concentration of sand at and beyond the former offlap breaks indicates that the clinoformed shelf margin was constructed mainly by welding of successive deltas that periodically spilled over the shelf edge and fed turbidites located on the slope itself and down to its toe.

Sequence stratigraphic framework

A prevailing depositional motif in the stratigraphic architecture of the Chodenice and Grabowiec clinoforms is a coarsening-upward unit interpreted to reflect progradation of a deltaic shore (Fig. 10). Because of the predominantly geophysical nature of the database available, a sequence stratigraphic framework for the upper Badenian-lower Sarmatian supra-evaporite succession was based on the nature of stratal lap outs seen of the seismic record and on parasequence stacking patterns, tied to the foraminiferal and nannoplankton zonation (Fig. 4).

Unconformities and sequences boundaries

Five types of unconformity have been distinguished in the studied clinoforms (Fig. 11). The most common are (A) internal downlap unconformities that partition the clinoform into individual stacked and laterally offset clinoform sets. However, many such unconformities appear to have only local ex-

Fig. 11. Summary of stratal lap-out patterns derived from the seismic record.

tent. This may reflect autocyclic changes in progradation direction or in the process regime affecting the deltas. It has been demonstrated on high-resolution seismic data from Pleistocene deltaic shelf margins that such *internal* downlap surfaces can have a regional persistence, and reflect minor drops and stillstands within the overall falling relative sea level (Kolla et al. 2000; Tesson et al. 2000). In the present instance, no such persistence could be demonstrated for the internal downlap surfaces. Seven (B) regional downlap unconformities that pass through the shaly intervals were mapped throughout the area, and interpreted as main flooding surfaces (MSF).

(C) Another type of unconformity is expressed on the shelf margin as an erosion surface below a blocky sandstone; this surfaces passes downdip beneath steep (3–4°) planar to oblique-tangential strata composed of aggrading thick-bedded massive sandstones (Fig. 10A, SB3 between wells Krz-2 and Pu-6). In some instances, the sandstones can be demonstrated to onlap upslope onto this unconformity. An erosional unconformity below a sharp-based sandstone on the shelf can also pass on the slope into either (D) a downlap unconformity beneath a prograding mouth-bar, or (E) an onlap unconformity that separates a prograding mouth-bar complex below from an aggrading to backstepping one above (Fig. 11). In the latter instance, such a turnover surface can be marked below by a downward shift in onlap (Figs. 11 and 12). In some instances, however, it is unclear, due to insufficient seismic resolution, whether the turnover surface merges with the base or with the *top* of the sharp-based sandstone.

Among the unconformities listed above, types C to E are potential candidates for sequence boundaries (SB), because they are associated with regional erosional truncation and/or basinwards facies shift. Types C and D conform to the Exxonian type 1 unconformity (Van Wagoner et al. 1990). Type E (turnover surface) appears to merge upslope into the type D unconformity. This reflects a more general dilemma as to whether a master sequence boundary should be placed at the base of prograding complex (Posamentier & Morris 2000), or at its top (Plint & Nummedal 2000). The latter approach was attempted here. Sequence boundaries SB2 and SB3 are similar in that they are associated with relatively thin, sharp-based sandstones that tend to pinch-out rapidly landwards within shelf shales and are underlain by thick-bedded massive sandstones onlapping back onto the slope (Fig. 10). Sequence boundary SB3 appears to be associated with a valley that dissected the shelf edge (Figs. 7B and 10A). SB1 could not be traced landwards into the shelf realm because it is cut by the frontal thrust of the Zgłobice Unit. This boundary is overlain by thick-bedded massive sandstones and hence, is probably of the same character as SB2 and SB3. Sequence boundary SB4 coincides with the erosive base of the Bogucice Sand tongue representing the basal member of the Chodenice Beds (Fig. 4). Farther to the southwest, this surface follows the base of a valley system (Skoczylas-Ciszewska & Kolasa 1959; Porębski & Oszczypko 1999) that still further landwards cuts down into the uplifted substratum (Garlicki 1968). The valley incision probably did not reach the coeval shelf break. On the slope, SB4 appears to correlate with a turnover surface that
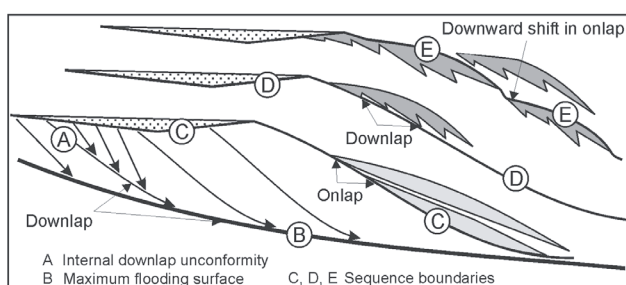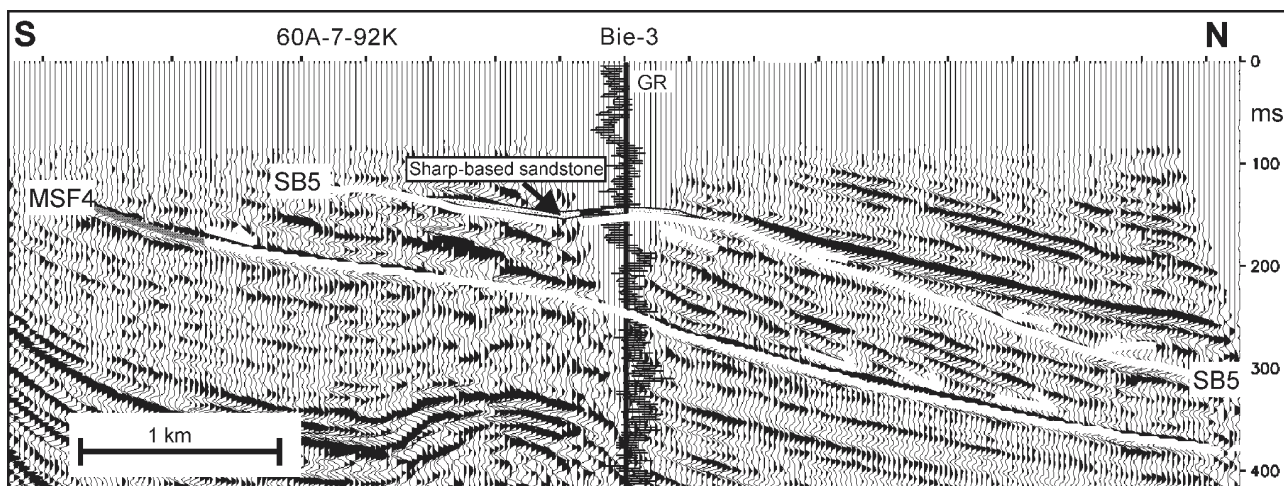
Fig. 12. Portion of a seismic dip-line showing the updip transition of onlap (turnover) onto the SB5 unconformity on the slope into the sharp-based sandstone at the shelf edge.

separates an upper backstepping mouth-bar set from a lower progradational set (Fig. 10A). Sequence boundaries SB5 and SB6 display a similar character (Fig. 10B). Sequence boundary SB7 was mapped only in the northeastern corner of the study area, where it appears as toplap truncation surface below a major valley (Fig. 9) that breached the former shelf edge (Fig. 7F).

Depositional sequences

In total, six 4th-order depositional sequences have been distinguished within the stratigraphic framework of upper Badenian-lower Sarmatian strata (Fig. 4). Each sequence forms a northward thinning wedge that displays a sigmoidal shape in dip cross-section, with the thickest part located immediately at or below the former shelf edge (Fig. 13). The six sequences are stacked vertically to form an offlapping prism, within

which the distal pinch-outs prograded some 15 km northwards during the time span involved (Fig. 13).

Transgressive systems tracts (TST) overlie a regional maximum regressive surface (MRS) and are characterized by a modest thickness (<20 m thick in the area landwards of the shelf edge) and by major shoreline backstep (generally greater than the preserved width of the shelf). Deposits in these tracts include plankton-enriched shales in the basinal realm and marine mudstones and prodeltaic heteroliths on the shelf. Transgressive shoreface or deltaic sands are remarkably rare. Highstand systems tracts (HST) tend to be thick and shaly on the shelf, but their thickness decreases upwards through the succession. Highstand deposits include mainly marine shale and progradational deltaic deposits, and there is a remarkable lack of paralic coastal-plain deposits within the study area. Deposits assigned to forced regressive systems tracts (FRST) include prograding mouth bars that show landward pinch-outs
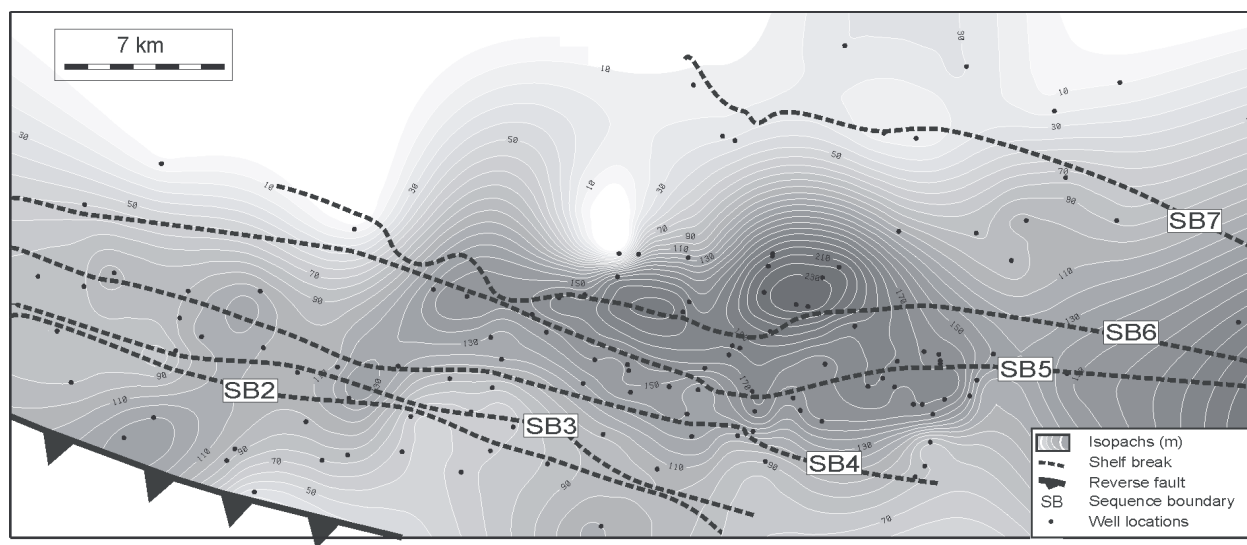
Fig. 13. Thickness map of depositional sequence S4 and the successive locations of the shelf break during progradation of the clinoforms.
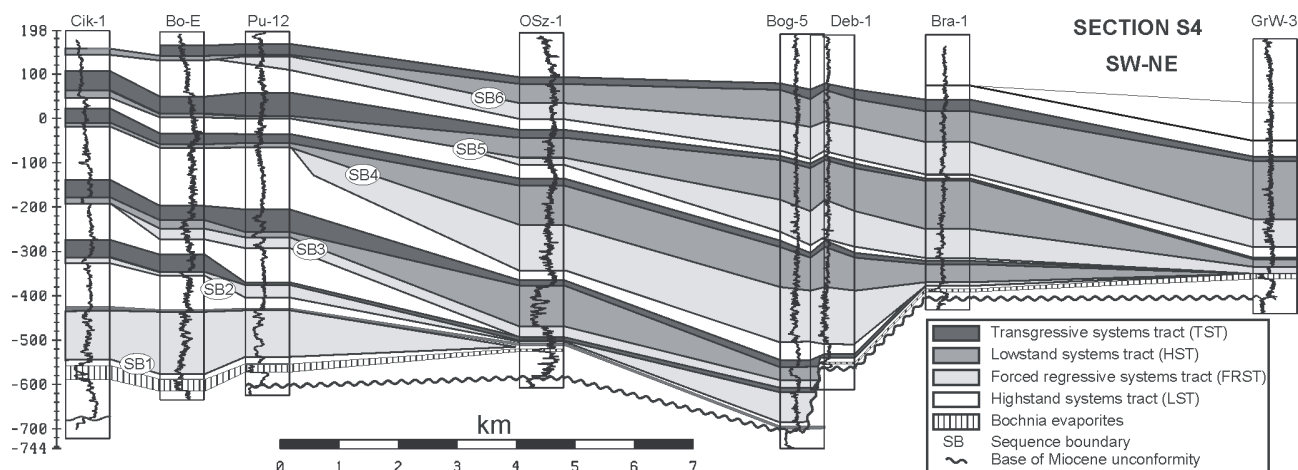
Fig. 14. Interpretation of depositional systems tracts in selected dip cross-sections.

by onlap back towards the shelf and pass basinwards into thin-bedded prodelta/slope heteroliths locally intercalated with thick-bedded blocky sandstones. Lowstand systems tracts are characterized within the slope either by thick-bedded blocky sandstones, or aggrading to backstepping deltaic mouth bars, or both. Thin (less than 30 m) blocky to fining-upwards sandstones located on the shelf have been interpreted as valley fills, although some blocky unit may in fact represent forced regressive mouth bars. The inferred valley fills (Fig. 9) may contain either fluvial or estuarine deposits; in the latter case, these fills should rather be included within transgressive systems tract (comp. Mellere & Steel 1995).

Forced regressive systems tract

The systems tract assignment of forced regressive deposits and the stratigraphic position of the associated sequence boundary are still a matter of controversy (Posamentier & Morris 2000). However, there is a growing consensus that deposits formed during the fall of relative sea level should not be lumped together with those formed during the sea-level rise, but warrant a distinction within a separate, forced regressive or falling-stage systems tract (Hunt & Tucker 1992, 1995; Mellere & Steel 1995; Plint & Nummedal 2000). The base of the forced regressive systems tract should be placed at the first downlap surface recording initial sea-level drop from its maximum highstand (sequence boundary *sensu* Posamentier & Morris 2000; see also Posamentier et al. 1992). In the present case, however, the proximal part of the systems tracts is not preserved; hence, the positions of the highstand shorelines are uncertain. Therefore, it is difficult to evaluate whether the *first observed* downlap surface, or the bypass zone between downdip detached mouth bars, reflects the initial drop in relative sea level from its highstand location, or a pulse within the already falling sea level, as exemplified by Pleistocene eustatic stepwise fall (e.g. Kolla et al. 2000). Nonetheless, a distinction of the forced regressive systems tract was attempted during well correlations (Fig. 14). For mapping purposes, however, highstand and forced-regressive deposits were included within a single tract (HST–FRST). In the approach adopted

here, the sequence boundary is placed at the base of onlapping, thick-bedded slope turbidites (Fig. 11) and where these are absent, at the turnover from the progradational to retrogradational parasequence sets within the slope realm (Fig. 10). In both cases, the sequence boundary defined in this way can commonly be seen to pass into the base of sharp-based sandstones inboard of the shelf (e.g. Fig. 14).

Depositional systems tracts and paleogeography

The lowstand systems tract in sequence S1 (LST1) forms two depocentres (Fig. 15A). The southwestern depocentre is a slope-toe linear wedge, 4 km wide and over 100 m thick, which is built mainly of thick-bedded turbidite sandstones that downlap onto the top of the Bochnia evaporites (Fig. 10). The other depocentrum consists of similar sand turbidites that fill and onlap from the south the SE-plunging Szczurowa Valley incised into the basement (Figs. 3 and 15B). The top of the Bochnia Formation is interpreted as a maximum flooding surface (MFS0) because of the deep-water nature of the evaporites (Peryt 2000) and, because they are immediately overlain by pteropod-bearing shales that represent a deep-water basinal facies. Sequence 1 has a very thick (75–125 m) highstand and forced-regressive systems tract (HST–FRST1) that is dominated by mud-prone sediment and has a maximum flooding surface (MFS1) associated with radiolaria-bearing shales (Fig. 4). At its very top there occurs a prograding sandbody, interpreted as a forced regressive mouth bar, that extends 15 km along the WNW-ESE trending shelf edge (Fig. 15B). It wedges outs downdip into rather gently dipping slope mudstones that are overlain (across a sequence boundary) by hyperpycnal turbidites of LST2 (Fig. 15C). The turbidites form a fan-shaped body, up 60–70 m thick and 14 km wide along the strike. The body was derived from the southeast and was in a large part ponded in a slope mini-basin located between growth anticlines (Fig. 15C).

The mud-prone HST–FRST2 has near its top a thin series of prograding to downstepping mouth bars striking WNW-ESE that wedge out downdip at the former shelf break (Fig. 15D).
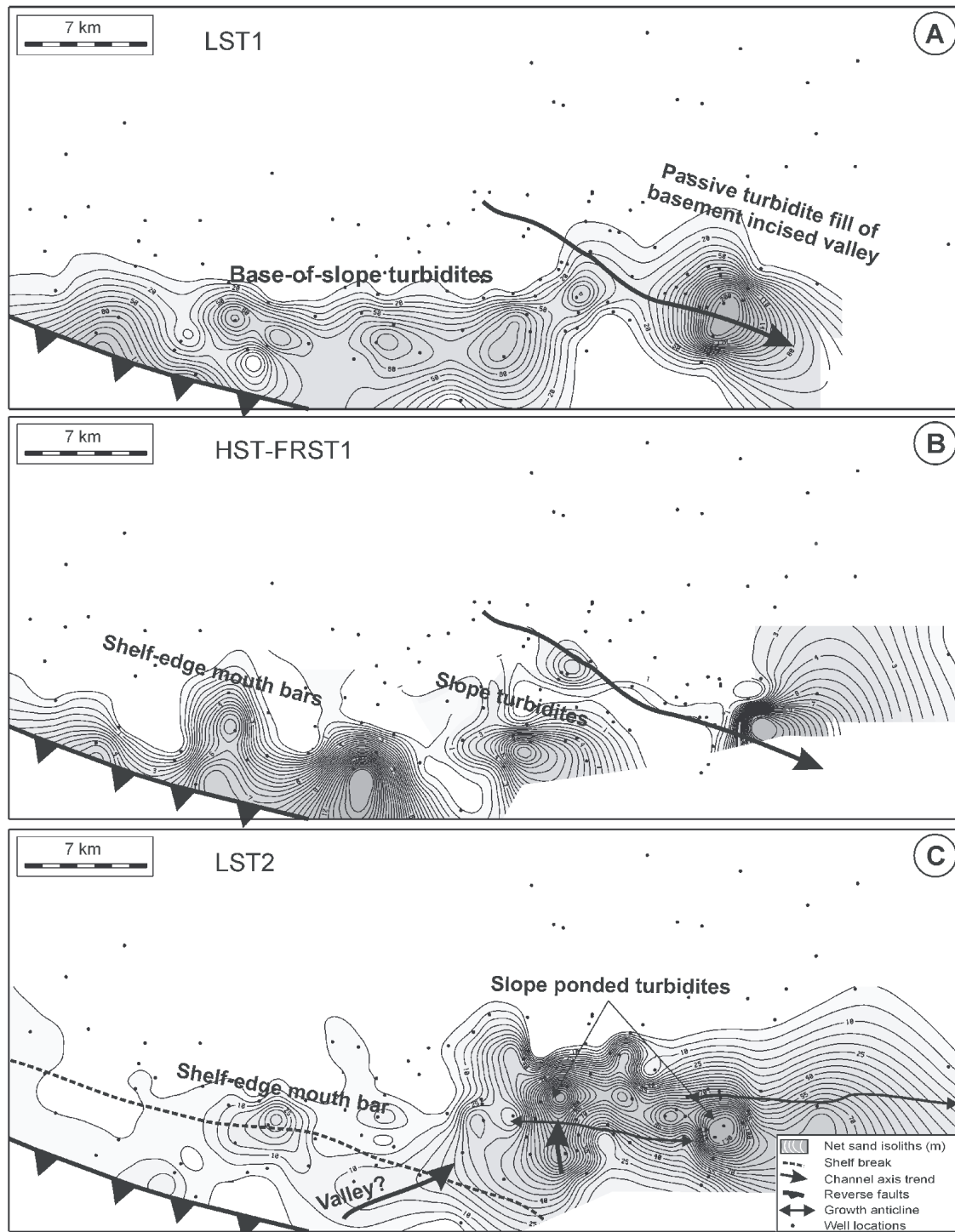
Fig. 15A,B,C. *Continued on pages 131, 132 and 133.*

LST3 is typified by a thick (over 100 m) accumulation of thick-bedded hyperpycnal turbidites that form an aggrading linear body, up to 30 km in strike dimension on the slope (Fig. 15E). Part of this body was trapped in a mini-basin on the slope behind a growing anticline, and extends updip for 5.5 km (comp. Fig. 7B). At, and landwards of the WNW-ENE striking shelf edge, there occur a series of aggrading to retreating mouth bars that farther to the SW appear to pinch out by onlap within shelf shales. A valley fill, up to 30 m thick, underlies these mouth bars, and appears to have breached the shelf break near its western end (Fig. 15C).

HST–FRST3 has a more heterolithic aspect than the previously described highstand to forced-regressive systems tracts. Within the shelf realm these heteroliths coarsen upwards into a sandstone whose top is planar to slightly descending basinwards (Figs. 10 and 15F) that is characteristic for forced re-
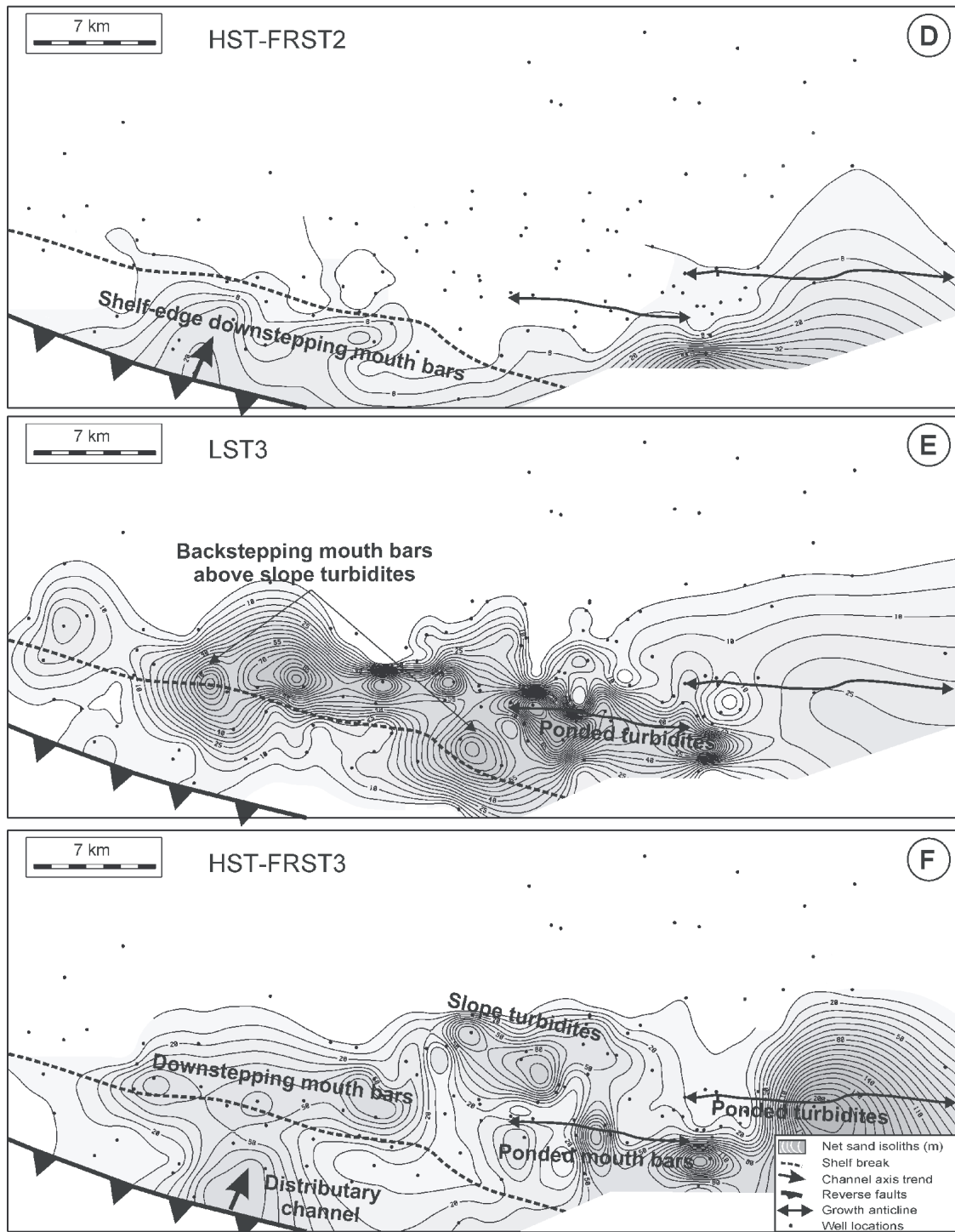
Fig. 15D,E,F. *Continued on pages 132 and 133.*

gression (Plint & Nummedal 2000). This sand belt trending WNW-ESE is formed of prograding mouth bars that descended onto the slope and were in part ponded in the slope mini-basin (Fig. 15F). A NNE-SSW striking finger-like sandbody in the SW part of the area may represent the fill of a distributary channel or valley. The mouth bars are separated basinwards by muddy slope sediments from another sand belt interpreted as slope-toe thin-bedded turbidites. Both sand belts,

together with the intervening slope mudstones, are interpreted as forced regressive deposits.

The overlying LST4 consists of a series of NW-striking mouth bars that are arranged in a backstepping fashion, and reveal the highest net sand content just landwards of the former shelf break, and are partly trapped behind rising anticlines piercing the slope in the eastern part of the area (Figs. 15G and 7C). At their landward onlap termination, the bars
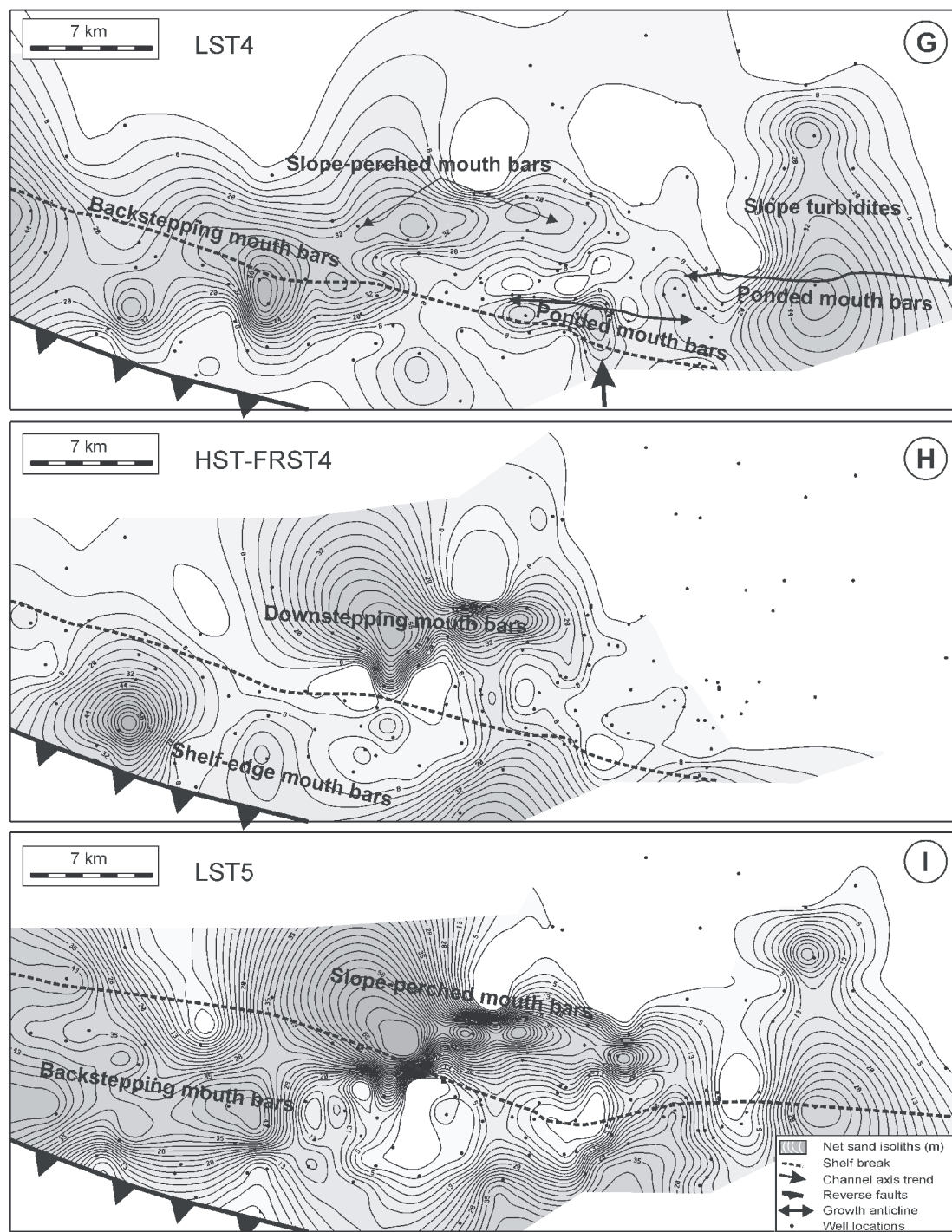
Fig. 15G,H,I. *Continued on page 133.*

appear to be dissected by channel feeders. West of the study area, this unit is based by a major incised valley system (Porębski & Oszczypko 1999), which apparently did not reach the former shelf edge. HST–FRST4 is thin and sandy landwards of the shelf edge and could in fact be entirely classified as a forced regressive systems tract. This unit is typified by an E-W-trending perched mouth bar that descended for 5–6 km down the slope; its landward pinch-out is located just beyond the shelf edge (Fig. 15H). The bar is separated by a 10–11 km bypass zone from the preceding (highstand?) mouth-bar edge (Fig. 15H).

LST5 in turn, displays mouth bars that aggraded on the slope and retreated 8–9 km from the newly formed shelf edge (Fig. 15I). HST–FRST5 displays a narrow belt of mouth bars located just around the shelf break (Fig. 15J). LST6 is typified by backstepping mouth bars that are backed updip by finger-like N-S to NW-ESE trending fills of feeder channels (Fig. 15K). This tract is bounded at its top by a NE-SW strik-
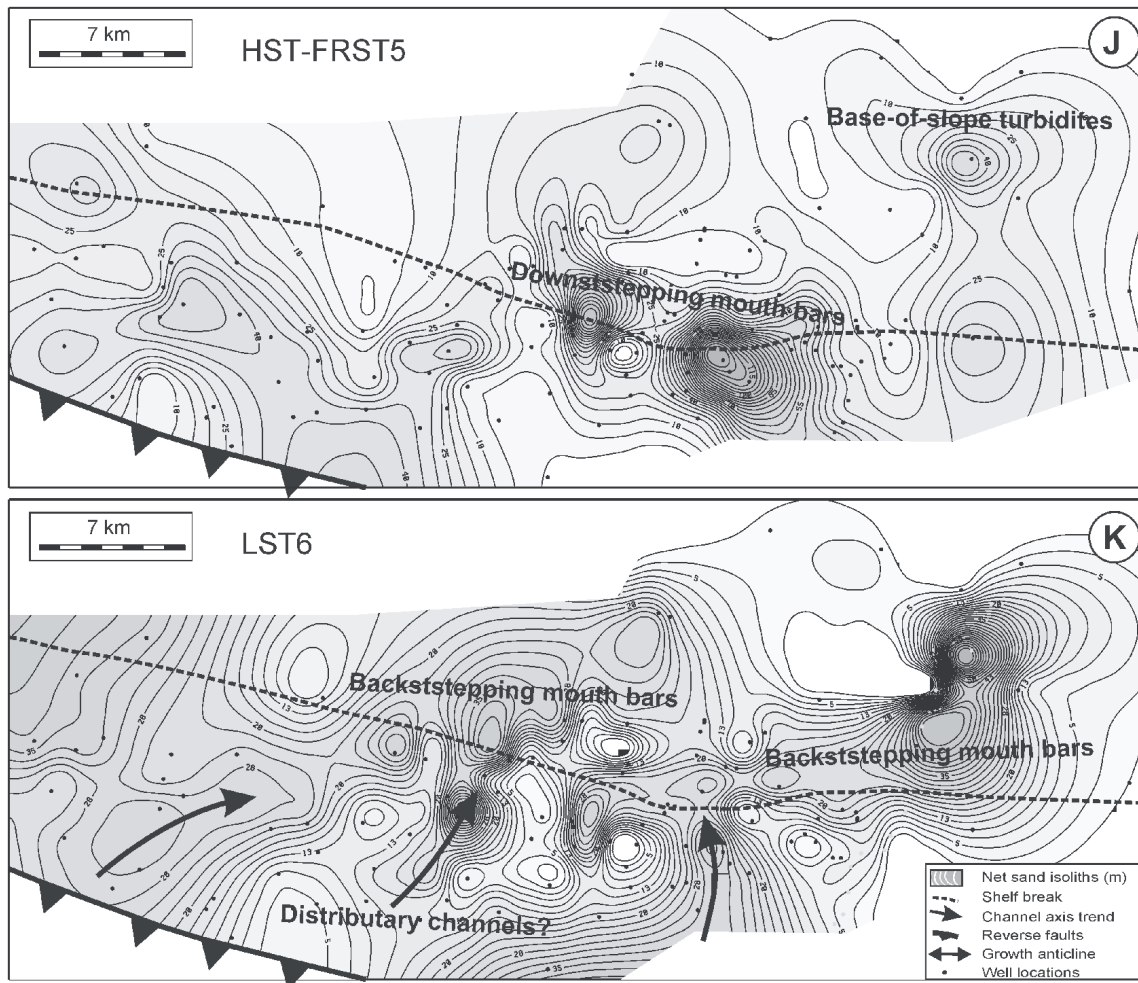
Fig. 15. Net-sand isolith maps with paleogeographic interpretation added, showing clinoform evolution for lowstand systems tracts (LST) and combined highstand and forced regressive systems tracts (HST–FRST). (***Fig. 15 begins on page 130.***)

ing valley system (Fig. 10). Only the northeastern part of this system was mapped here (Fig. 7F), because its proximal part lies above the upper limit of the seismic record.

Clinoform types

Two end members in the large-scale clinoform architecture can be distinguished within the studied shelf margin (Fig. 16). Type A clinoform is characterized by a steep, (3–4°) and narrow (2–4 km) slope of a relatively low height (150–200 m). Slope sediments are dominated by thick-bedded massive sandstones that show downlapping lower ends and onlapping upper terminations. The coeval shelf margin can locally be dissected by distributary channels or incised valleys. Such shelf-margin architecture appears to have developed during the maximum fall and early rise in relative sea level.

The Type B clinoform is less steep (2°), tangential in cross-section and wide (>12 km), and shows a considerable height (up to 400 m). Clinoform strata are constructed mainly of mouth bars perched on the slope. These show initially a pro-gradational to downstepping arrangement over a distance of

6–10 km downdip from the former shelf edge; this pattern is followed by a rise and landward migration of the offlap breaks (comp. Fig. 10). Thick-bedded massive sandstones bodies are noticeably absent, although thicker, shingled turbidites can locally be present, being associated mainly with the downstepping segment of the shelf-edge trajectory. There is no evidence for shelf edge dissection accompanying the development of this type of shelf-margin architecture. The Type B clinoforms are formed during a stepwise fall and early rise in relative sea level.

Although no basin-floor fan was documented within the limits of the study area, it is predicted that such fan deposits may develop basinwards of the Type A clinoforms, provided the initial slope downdip width was sufficiently large (larger than that documented here) to ignite low-density turbidity currents from river-born hyperpycnal flows (see below).

Lower-order sequences

The six 4th-order sequences described are stacked basin-wards and vertically to form an aggradational to pro-
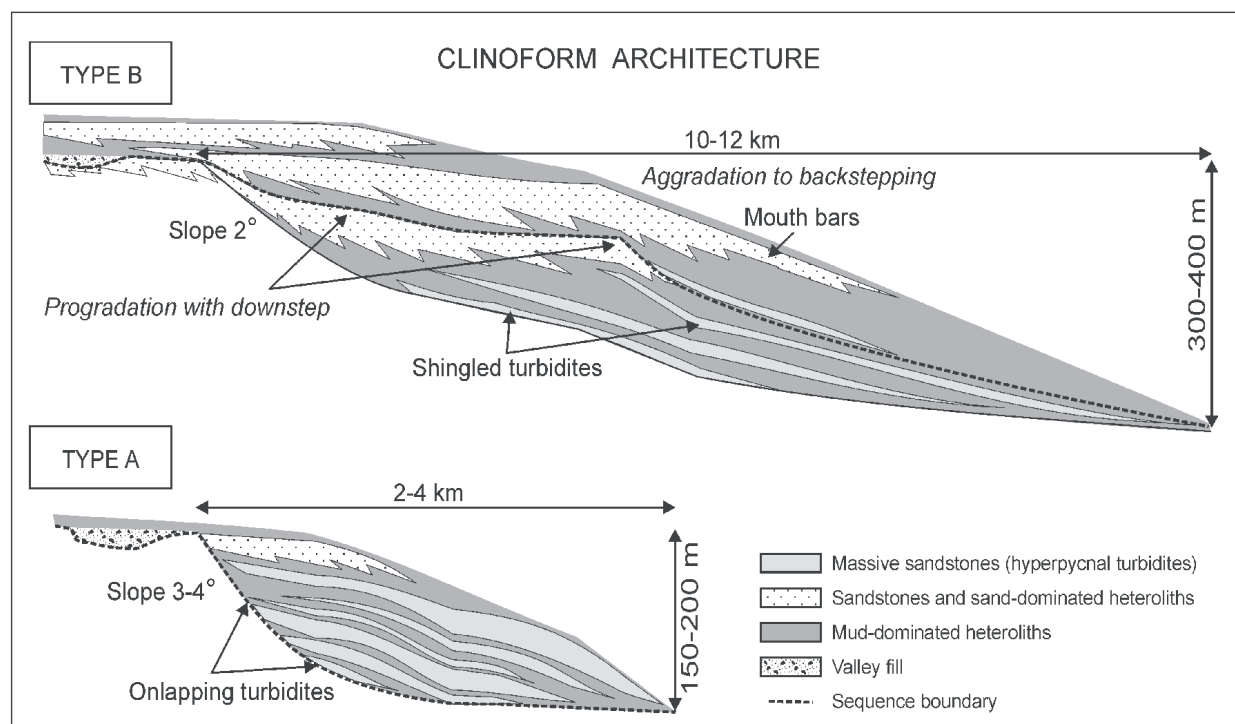
Fig. 16. Summary of main types of clinoform architecture.

gradational succession that get sandier both upwards and basinwards. Two 3rd-order sequences have been distinguished within the succession (Fig. 4). The lower sequence (Ba2, upper Badenian) consists of sequences 1 to 3, and its upper boundary is defined at the base of valley system that underlies the Bogucice Sand tongue. The upper sequence (Sa1; lower Sarmatian) consists of sequences 4 to 6; its top has tentatively been placed at the surface SB7 associated with a valley system.

Sequence Ba2 consists of Type A clinoform bundles in which the offlap break rises steeply basinwards throughout the development of the component high-order sequences (Fig. 10). This is associated with thick, mud-prone transgressive and highstand systems tracts landwards of the shelf break, with the highstand tracts commonly capped by thin forced regressive mouth-bar/shoreface sands. Lowstand tracts are typified by thick massive turbidites deposited on a narrow, steep slope, and their maximum strike extent is 14–30 km. In some instances (LST3 and possibly LST2), the slope turbidites appear to be linked up dip to valleys that breached the shelf edge (Fig. 15C). The slope is locally affected by anticlines that grew above the tips of blind thrusts. The resultant mini-basins perched on the slope acted as traps for hyperpycnal turbidites and mouth bars spilling over the shelf edge.

From sequence boundary SB4 on, the shelf break recurrently assumes a noticeably flatter trajectory basinwards (Fig. 10), and the shelf margin grew mainly through the accretion of Type B clinoform bundles. Landwards of the shelf break, transgressive and highstand systems are either thin, or absent, whereas prograding to downstepping mouth bars form the bulk of forced regressive systems tracts. Slope-perched mouth bars that aggraded and stepped back onto the shelf typify lowstand tracts. Although the feeder system was intermittently able to arrive close to the shelf edge, there is evidence of a major incision into the shelf edge only for one sequence boundary (SB7) (Fig. 7F).

Discussion and conclusions

The best-known examples of shelf-margin or deep-water deltas (Edwards 1981) are those described from the Pleistocene of the modern continental shelf edges (e.g. McMaster et al. 1970; Suter & Berryhill 1985; Tesson et al. 1990, 2000; Kolla et al. 2000). It is commonly believed that deltaic progradation across the shelf to its margin is caused by either forced regression during relative sea-level fall (e.g. Posamentier et al. 1992), or anomalously large siliciclastic sediment influx (Poag & Sevon 1989).

It is suggested here that the bathymetric step for such deep-water deltas does not need to be the topographic break inherited after extensional faults or rifting, as is commonly the case for modern divergent margins. Such a topographic or shelf-edge break can also be the constructional brink where successive shelf-transiting deltas encounter and descend into a deep basin. This type of constructional shelf edge is created by repeated regressive–transgressive transit of deltas. The shelf has its maximum width during sea-level highstand, and can have zero width at lowstand, when delivery of sediment causes renewed shelf-margin accretion.

In the present case, the initial shelf break was nucleated along a thrust or thrust-generated anticlinal front located southwards from the present basin margin. During the earliest Badenian, this front was probably situated some 30 km south of the Carpathian overthrust, as suggested in the palinspastic

restoration by Oszczypko (1997, his Fig. 15). This may possibly represent a crude estimate of the position of highstand shorelines with respect to the coeval shelf margin. The latest Badenian-early Sarmatian thrusting resulted in growth anticlines affecting the clinoform body, which led to a steepening of its slope. A strongly aggradational character to shelf-margin deltas, as observed in the lower clinoform set (sequence Ba2), appears incompatible with the striking absence of paralic deposits. This is because a climbing clinoform trajectory caused by relative sea-level rise tends to generate space behind, where a thick 'tail' of paralic deposits can be accommodated. However, the absence of such a tail in the present instance reflects a modest to negative accommodation behind the rising thrust margin, whereas subsidence in the hangingwall created enough space to accommodate steep and high clinoforms.

Shelf-margin deltas appear to record periods when the sediment is stored at the shelf edge rather than is being delivered into the deep water. The difference between the two clinoform end-member types distinguished here seems to have been controlled chiefly by rate of relative sea-level change that governed the position of the seaward end of the feeder system with respect to the former shelf break, although differences in depositional regimes on the outer shelf could also have played a significant role (cf. Steel et al. 2000). The sand-prone Type A clinoforms appear to record a situation when the feeder system incised across the shelf edge in response to a rapid relative fall in sea level. This caused cannibalisation of the previous shelf deltas and promoted fluvial input directly onto the slope. The resultant hyperpycnal flows came to rest on the slope itself, probably because the small downdip width of the slope and the presence of perched basins prevented flow ignition into high-efficiency turbidity currents capable for transporting sand into the basin-plain area. The composite, heterolithic Type B clinoforms record initially rather slow and stepwise fall in relative sea level. Incision of the feeder-channel system progressed gradually behind the prograding deltaic shelf margin (comp. Sydow & Roberts 1994), but was apparently unable to breach the freshly accreting shelf edge even during the maximum lowstand. During early sea-level rise, aggradation followed by backstepping of deltas took place. Therefore, the development of Type B clinoform sets documents trapping of sand within deltaic depocentres that shifted forth and back on the slope and, consequently, a decreased probability for sand to escape into the basin-floor setting.

The change from the steeply rising to a more horizontal trajectory of the shelf margin, together with the compressional setting of the studied clinoform, points to a major change in the tectonic component in the relative sea-level signal during the clinoform growth. The particularly strong aggradation and the large thickness of the upper Badenian highstand systems tracts (sequences 1 to 3) point to strong differential movements across a N-verging thrust-fault margin, that generated a long-term relative sea-level rise on the hangingwall. The period of fault-induced subsidence ended with the latest Badenian-early Sarmatian uplift to the southwest. Since then, high-frequency relative sea-level fluctuations were superposed on a less vigorous regional flexural subsidence pattern, that resulted in faster accretion and increased width of the clinoforms (sequences 4 to 6).

References

Alexandrowicz S.W. 1997: Lithostratigraphy of the Miocene Deposits in the Gliwice Area (Upper Silesia, Poland). *Bull. Pol. Acad. Sci. Earth Sci.* 45, 167–179.

Bukowski K. 1999: Comparison of the Badenian saliferous series from Wieliczka and Bochnia in light of new data. *Prace Państw. Inst. Geol.* 168, 43–51 (in Polish, English summary).

Czapowski G. 1994: Sedimentation of Middle Miocene marine complex from the area near Tarnobrzeg (north-central part of the Carpathian Foredeep). *Geol. Quaterly* 38, 577–592.

Czepiec I. & Kotarba M.J. 1998: Paleoecology and organic matter in the Late Badenian and Early Sarmatian marine basin of the Polish part of the Carpathian Foredeep. *Przegl. Geol.* 46, 32–736.

Edwards M.B. 1981: Upper Wilcox Rosita delta system of South Texas: growth-faulted shelf-edge deltas. *Amer. Assoc. Petrol. Geol. Bull.* 65, 54–73.

Garecka M. & Jugowiec M. 1999: Results of biostratigraphic study of Miocene in the Carpathian Foredeep based on calacareous nannoplankton. *Prace Państw. Inst. Geol.* 168, 29–41 (in Polish, English summary).

Garlicki A. 1968: Autochthonous salt series in the Miocene of the Carpathin Foredeep between Skawina and Tarnów. *Biul. Inst. Geol.* 215, 5–61 (English summary).

Garlicki A. 1994: Formal lithostratigraphic units of the Miocene: Wieliczka Formation. *Przegl. Geol.* 42, 26–28 (in Polish, English summary).

Gonera M. 1994: Paleoecology of marine Middle Miocene (Badenian) in the Polish Carpathians (Central Paratethys). Foraminiferal record. *Bull. Pol. Acad. Sci. Earth Sci.* 42, 107–125.

Hunt D. & Tucker M.E. 1992: Stranded parasequences and the forced regressive wedge systems tract: deposition during base-level fall. *Sed. Geol.* 81, 1–9.

Hunt D. & Tucker M.E. 1995: Stranded parasequences and the forced regressive wedge systems tract: deposition during base-level fall. *Sed. Geol.* 95, 147–160.

Jasionowski M. 1997: Lithostratigraphy of the Miocene deposits in the eastern part of the Carpathian Foredeep. *Biul. Państw. Inst. Geol.* 375, 44–60 (in Polish, English summary).

Karnkowski P.H. & Ozimkowski W. 2001: Structural evolution of the pre-Miocene basement in the Carpathian Foredeep (Kraków-Przemyśl region, SE Poland). *Przegl. Geol.* 59, 431–436 (in Polish, English summary).

Kasprzyk A. 1993: Lithofacies and sedimentation of the Badenian (Middle Miocene) gypsum in the Northern part of the Carpathian Foredeep, Southern Poland. *Ann. Soc. Geol. Pol.* 63, 33–84.

Kirchner Z. 1956: Miocene stratigraphy of the Central Carpathian Foreland based on microfaunal studies. *Acta Geol. Pol.* 6, 421–449 (in Polish, English summary).

Kolla V., Biondi P., Long B. & Fillon R. 2000: Sequence stratigraphy and architecture of the Late Pleistocene Lagniappe delta com-

plex, northeast Gulf of Mexico. In: Hunt D. & Gawthorpe R.L. (Eds.): Sedimentary responses to forced regressions. *Geol. Soc. London, Spec. Publ.* 172, 291–327.

Kotarba M.J., Wilczek T., Słupczyński K., Kosakowski P., Kowalski A. & Więcław D. 1998: A study of organic matter and habitat of gaseous hydrocarbons in the Miocene strata of the Polish part of the Carpathian Foredeep. *Przegl. Geol.* 46, 742–750.

Kotlarczyk J. 1985: An outline of the stratigraphy of marginal tectonic units of the Carpathian orogen in the Rzeszów-Przemyśl area. *Carpatho-Balkan Geological Association XIII Congress,* Cracow, Poland, *Guide to excursion* 4, 39–64.

Krzywiec P. 1997: Large-scale tectono-sedimentary Middle Miocene history of the central and eastern Polish Carpathian Foredeep Basin — results of seismic data interpretation. *Przegl. Geol.* 45, 1039–1053.

Kuciński T.M. 1982: A contribution to the stratigraphic framework of the Miocene in southern Poland. *Kwart. Geol.* 26, 471–472 (in Polish).

Łuczkowska E. 1964: The micropaleontological stratigraphy of the Miocene in the region Tarnobrzeg-Chmielnik. *Prace Geol. PAN* 20, 1–71.

Łuczkowska E. 1995: Biostratigraphic correlation of new wells drilled in the Miocene of the Wieliczka area. *Geologia AGH* 21, 255–265 (in Polish).

Mayall M.J., Yeilding C.A., Oldroyd J.D., Pulham A.J. & Sakurai S. 1992: Facies in a shelf-edge delta — an example from the subsurface of the Gulf of Mexico, middle Pliocene, Mississippi Canyon, Block 109. *Amer. Assoc. Petrol. Geol. Bull.* 76, 435–448.

Maksym A., Liszka B., Staryszak G. & Dziadzio P. 1997: Depositional model of the Badenian-Sarmatian sandstone in the Carpathian Foredeep (autochthonous Miocene, Husów-Albigowa-Krasne). *Konferencja Naukowo-Techniczna pt. „Zespołowa Analiza Geologiczna Źródłem Postępu w Poszukiwaniach Naftowych",* Warszawa, 171–173.

McMaster R.L., de Boer J. & Ashraf A. 1970: Magnetic and seismic reflection studies on Continental Shelf off Portuguese Guinea, Guinea, and Sierra Leone, West Africa. *Amer. Assoc. Petrol. Geol. Bull.* 54, 158–167.

Mellere D. & Steel R.J. 1995: Variability of lowstand wedges and their distinction from forced regressive wedges in the Mesaverde Group, southeast Wyoming. *Geology* 23, 803–806.

Ney R. 1968: The role of the Cracow Bolt in the geolofical history of the Carpathian Foredeep. *Prace Geol. Kom. Nauk Geol. PAN Oddz. w Krakowie* 45, 1–82 (in Polish, English summary).

Olszewska B. 1999: Biostratigraphy of Neogene in the Carpathian Foredeep in light of new micropalaeontological data. *Prace Państw. Inst. Geol.* 168, 9–28 (in Polish, English summary).

Oszczypko N. 1997: The Early-Middle Miocene Carpathian peripheral foreland basin (Western Carpathians, Poland). *Przegl. Geol.* 45, 1054–1063.

Oszczypko N. & Żytko K. 1987: Main stages in the evolution of the Polish Carpathians during Late Paleogene and Neogene times. In: Leonov Y.G. & Khain V.E. (Eds.): Global Correlation of Tectonic Movements. *John Wiley & Sons Ltd.*, 187–198.

Peryt T.M. 2000: Resedimentation of basin centre sulphate deposits: Middle Miocene Badenian of Carpathian Foredeep, southern Poland. *Sed. Geol.* 134, 331–342.

Picha F.J. 1996: Exploring for hydrocarbonds under thrust belts a challenging new frontier in the Carpathians and elsewhere. *Amer. Assoc. Petrol. Geol. Bull.* 80, 1547–1564.

Plink-Bjorklund P., Mellere D. & Steel R.J. 2001: Turbidite variability and architecture of sand-prone, deep-water slopes: Eocene clinoforms in Central Basin, Spitsbergen. *J. Sed. Res.* 71, 895–912.

Plint A.G. & Nummedal D. 2000: The falling stage systems tract: rec-

ognition and importance in sequence stratigraphic analysis. In: Hunt D. & Gawthorpe R.L. (Eds.): Sedimentary Responses to Forced Regressions. *Geol. Soc. London, Spec. Publ.* 172, 1–17.

Poag C.W. & Sevon W.D. 1989: A record of Appalachian denudation in postrift Mesozoic and Cenozoic sedimentary deposits in the U.S. middle Atlantic continental margin. *Geomorphology* 2, 119–157.

Połtowicz S. 1997: The apparent onlap of Badenian strata on seismic sections. *Nafta – Gaz* 4, 117–125 (in Polish).

Połtowicz S. 1998: The Lower Sarmatian delta of Szczurowa on the background of the Carpathian Foreland geological evolution. *Geologia AGH* 24, 219–239 (in Polish, English summary).

Porębski S.J. 1999: Depositional setting of a supra-evaporate succession (Upper Badenian) in the Kraków-Brzesko area, Carpathian Foredeep Basin. *Prace Państw. Inst. Geol.* 168, 97–118 (in Polish, English summary).

Porębski S.J. & Oszczypko N. 1999: Lithofacies and origin of the Bogucice sands (Upper Badenian). *Prace Państw. Inst. Geol.* 168, 57–82 (in Polish, English summary).

Posamentier H.W. & Morris W.R. 2000: Aspects of the stratal architecture of forced regressive deposits. In: Hunt D. & Gawthorpe R.L. (Eds.): Sedimentary Responses to Forced Regressions. *Geol. Soc. London, Spec. Publ.* 172, 19–46.

Posamentier H.W., Allen G.P., James D.P. & Tesson M. 1992: Forced regressions in a sequence stratigraphic framework: concepts, examples, and exploration significance. *Amer. Assoc. Petrol. Geol. Bull.* 76, 1687–1709.

Roniewicz P. & Wysocka A. 1999: Sedimentology of the Middle Miocene deposits from the north-eastern marginal zone of the Carpathian Foredeep. *Prace Państw. Inst. Geol.* 168, 83–95 (in Polish, English summary).

Skoczylas-Ciszewska K. & Kolasa M. 1959: The Bogucice sands (Cracow area). *Ann. Geol. Soc. Pol.* 38, 285–314 (in Polish, English summary).

Steel R.J., Crabaugh J., Schellpeper M., Mellere D., Plink-Bjorklund P., Deibert J. & Loeseth T. 2000: Deltas versus rivers on the shelf edge: their relative contributions to the growth of shelf margins and basin-floor fans (Barremian and Eocene, Spitsbergen. *Proc. GCSSEPM Foundation 20th Annual Research Conference, Deepwater Reservoirs of the World*, Houston, 981–100.

Steel R.J., Mellere D., Plink-Bjorklund P., Porębski S.J. & Schellpeper M. 2001: Shelf-edge deltas: driver for shelf-margin accretion. *2001 AAPG Annual Convention June3-6, 2001,* Denver, Colorado, Official Program 10, A191.

Suter J.R. & Berryhill H.L. Jr. 1985: Late Quaternary shelf-margin deltas, northwest Gulf of Mexico. *Amer. Assoc. Petrol. Geol. Bull.* 69, 77–91.

Sydow J. & Roberts H.H. 1994: Stratigraphic framework of a Late Pleistocene shelf-edge delta, northeast Gulf of Mexico. *Amer. Assoc. Petrol. Geol. Bull.* 78, 1276–1312.

Ślączka A. & Kolasa K. 1997: Resedimented salt in the Northern Carpathians Foredeep (Wieliczka, Poland). *Slovak Geol. Mag.* 3, 135–155.

Tesson M., Posamentier H.W. & Gensous B. 2000: Stratigraphic organization of Late Pleistocene deposits of the western part of the Golfe du Lion Shelf (Languedoc Shelf), western Mediterranean Sea, using high-resolution seismic and core data. *Amer. Assoc. Petrol. Geol. Bull.* 84, 119–150.

Van Wagoner J.C., Mitchum R.M., Campion K.M. & Rahmani V.D. 1990: Silicilastic sequence stratigraphy in well logs, cores, and outcrops. *Amer. Assoc. Petrol. Geol. Methods in Exploration Series* 7, 1–155.

Żytko K. 1999: Correlation of the main structural units of the Western and eastern Carpathians. *Prace Państw. Inst. Geol.* 168, 135–164 (in Polish, English summary).